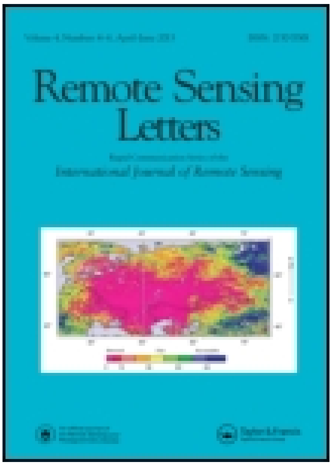

Remote Sensing Letters
Publication details, including instructions for authors and subscription information:
http://www.tandfonline.com/loi/trsl20

Use of simulated reflectances over bright desert target as an absolute calibration reference

Yves Govaerts [a] , Sindy Sterckx [b] & Stefan Adriaensen [b]
[a] Govaerts Consulting , Brussels , Belgium
[b] VITO, Centre for Remote Sensing and Earth Observation , Mol , Belgium
Published online: 05 Feb 2013.

Remote Sensing Letters, 2013
Vol. 4, No. 6, 523–531, http://dx.doi.org/10.1080/2150704X.2013.764026

Use of simulated reflectances over bright desert target as an absolute calibration reference

YVES GOVAERTS*†, SINDY STERCKX‡ and STEFAN ADRIAENSEN‡
†Govaerts Consulting, Brussels, Belgium
‡VITO, Centre for Remote Sensing and Earth Observation, Mol, Belgium

(*Received 10 October 2012; in final form 2 January 2013*)

This letter presents the improvements of an absolute calibration reference system based on simulated top-of-atmosphere bidirectional reflectance factor time series over bright desert targets. The current work highlights a case study performed over Committee on Earth Observation Satellites (CEOS) calibration target Libya4, demonstrating that it is possible to achieve a mean accuracy of 3% when simulation is compared with calibrated observations acquired by polar orbiting satellites.

1. Introduction

Project for On-Board Autonomy-Vegetation (PROBA-V) is a new European Space Agency (ESA) Earth Observation mission to be launched in 2013 dedicated to the global daily observation of land surfaces (Mellab 2009). Accurate calibration of images acquired by this satellite is critically important for the derivation of quantitative geophysical information on the state and evolution of vegetation. In this context, the Vlaamse Instelling voor Technologisch Onderzoek (VITO), who is responsible for PROBA-V user segment, has undertaken the development of an Optical Sensor CAlibration with simulated Radiance (OSCAR) facility for the routine vicarious calibration of space-based radiometers (Sterckx *et al.* 2012). The proposed approach relies on a combination of various vicarious calibration methods based on the exploitation of reflected radiance by clouds, atmospheric molecules and bright desert surfaces. The use of simulated reflectances over bright desert targets is a key component of this method which offers many advantages. Because of high surface reflectance of this type of surface, atmospheric contribution is small and the surface reflectance is very stable in time allowing consistent calibration with previous missions similar to PROBA-V such as VEGETATION-1 and VEGETATION-2 satellites.

Over bright desert targets, simulated top-of-atmosphere (TOA) bidirectional reflectance factors (BRFs) define an absolute reference against which radiometers can be calibrated or cross-calibrated. These simulations are based on the radiative properties originally proposed by Govaerts and Clerici (2004). Several improvements are presented here and concern (*i*) the use of an advanced radiative transfer model that accounts for polarization (Kotchenova *et al.* 2006, Kotchenova and Vermote 2007), (*ii*) the surface reflectance characterization and (*iii*) the use of a non-spherical aerosol model.

*Corresponding author. Email: ygovaerts@gmail.com

The purpose of this letter is to present these improvements and to evaluate the accuracy with which observations acquired by several polar orbiting imagers, presented in section 2, can be simulated. These improvements are described in section 3 and their evaluation in section 4. This work is performed in the framework of our contribution to Committee on Earth Observation Satellites/Working Group Calibration-Validation/Infrared Visible Optical Sensors (CEOS/WGCV/IVOS) calibration mission using data extracted from ESA Database for Imaging Multi-spectral Instruments and Tools for Radiometric Intercomparison (DIMITRI) (Bouvet and Ramoino 2010).

2. Satellite data

For the evaluation of the simulated TOA reflectance accuracy, a series of observations acquired by polar orbiting radiometers, i.e. VEGETATION-2, Polarization and Anisotropy of Reflectances for Atmospheric Sciences Coupled with Observations from Lidar (PARASOL), Envisat Medium Resolution Imaging Spectrometer (MERIS), Advanced Along-Track Scanning Radiometer (AATSR) and finally AQUA-MODIS have been processed. As can be seen in figure 1, the spectral responses of these instruments in the 0.4–1.8 μm region are located at different wavelengths and exhibits different width. Observations acquired by these instruments over Libya4 (Cosnefroy *et al.* 1997) during the 2006–2009 period have been extracted from the ESA DIMITRI database. Libya4 is a large sand dune area located at 23.39° N and

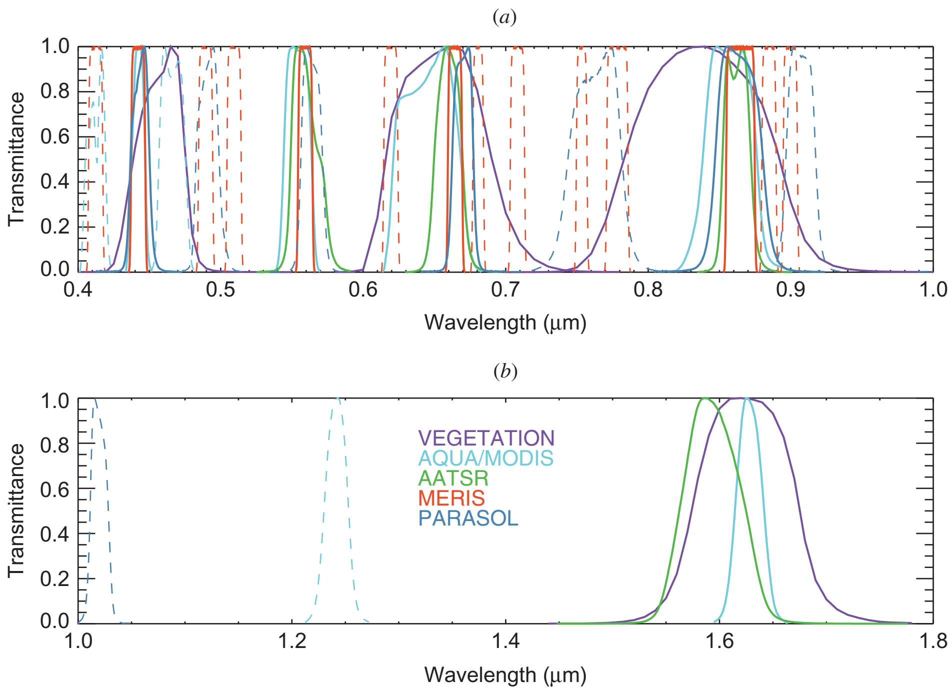

Figure 1. Sensor spectral responses of the VEGETATION-2, AQUA/MODIS, AATSR, MERIS and PARASOL radiometers used in this study. The common spectral bands are shown with thick solid lines (*a*) from 0.4 to 1.0 μm and (*b*) from 1.0 to 1.8 μm.

Table 1. Number of valid observations N_t in the common spectral bands during the 2006–2009 period over Libya4.

Bands (µm) sensors	0.44	0.55	0.66	0.84	1.62
VEGETATION	723	–	700	709	695
AATSR	–	114	117	119	120
PARASOL	4078	4072	4225	4205	–
MODISA	848	864	846	839	822
MERIS	371	378	372	367	–

28.55° E in the Sahara desert. The corresponding TOA BRFs acquired at time t have been simulated under the same geometry of observation Ω and accounting for the actual spectral response of each instrument. For each time series of the couple $(r_o(t,\Omega), r_s(t,\Omega))$, where $r_o(t,\Omega)$ and $r_s(t,\Omega)$ stand for the observed and simulated TOA BRF, respectively, the mean relative difference $\bar{B}$ and the standard deviation σ between these two distributions have been derived after removal of the outliers at a 2σ confidence interval. This test allows removing observations still contaminated by clouds. Almost all these radiometers observe approximately around the 0.44, 0.55, 0.66, 0.84 and 1.62 µm spectral regions that are referred to here as the common spectral bands. The number of valid observations in these bands, i.e. after removal of the outliers at 2σ, is indicated in table 1.

For the AATSR observations, only the nadir camera is considered in this study. For Moderate Resolution Imaging Spectroradiometer (MODIS), band B10 has not been processed because it sometimes saturates over Libya4. Finally, the oxygen band of MERIS and PARASOL has not been simulated because the Second Simulation of the Satellite Signal in the Solar Spectrum-Vector (SIXS-V) code does not have a spectral resolution high enough for accurate simulations in this region. Additionally, this model is not designed to simulate spectral regions exhibiting high absorption features.

3. Improved radiative transfer modelling

3.1 *Background*

The characterization of Libya4 surface radiative properties originally relies on the work of Govaerts and Clerici (2004). This characterization was based on few months of multi-angular spaceborne observations acquired by Advanced Earth Observation Satellite-1/Polarization and Directionality of Earth Reflectances (ADEOS-1/POLDER) in the 0.443, 0.670, 0.765 and 0.865 µm spectral bands and ESA Remote Sensing Satellite 2/Advanced Along-Track Scanning Radiometer 2 (ERS2/ATSR2) in the 1.6 µm band. The surface BRF model of Rahman *et al.* (1993), referred to as Rahman-Pinty-Verstraete (RPV), was inverted against these observations corrected from atmospheric scattering and absorption effects. Additionally, the ensemble of bright bare soil spectra of the Advanced Spaceborne Thermal Emission Radiometer (ASTER) spectral library (http://speclib.jpl.nasa.gov) matching these five spectral band values were used for the interpolation and extrapolation of the surface reflectance in the 0.4–1.8 µm spectral interval. TOA BRF simulations were performed with the SIXS-V code (Vermote *et al.* 1997), using the desert background aerosol model of Shettle and Fenn (1979) that assumes spherical particles.

3.2 *Radiative transfer model*

The improved radiative transfer simulations are now based on the SIXS-V code developed by Kotchenova *et al.* (2006). This code accounts for radiation polarization through the calculation of four components of the Stokes vector, i.e. $\boldsymbol{I} = \{I, Q, U, V\}$. The first component, I, describes the intensity of radiation; the other three characterize perpendicular Q, parallel U and elliptical V polarization. The scattering and absorption properties of aerosols are represented by the single scattering albedo ω_0 and the scattering matrix $\mathbf{P}(\Theta)$. This matrix describes the angular polarizing properties of a single-scattering event in the layer (Dubovik 2006).

3.3 *Surface characterization*

An updated version of the surface BRF data set has been generated taking advantage of the availability of more than 10 years of surface BRF values derived from MODIS (MOD09) and MISR (MISR-10) surface reflectance products (Diner *et al.* 1999, Vermote and Vermeulen 1999). For a given spectral band, when both MISR and MODIS data are available, only the MISR ones have been used. A new data set has therefore been generated using the approach described in section 3.1 and is shown in figure 2 with solid line. Both the shape of the BRF and the magnitude of the surface albedo are slightly different in this new data set. Currently, surface reflectance is assumed non-polarizing though typical polarization sand surface such as Libya4 is in the range of 0–15% (Liou 2002).

3.4 *Aerosol model*

An original method has been developed for the systematic analyse of AERONET data (Holben *et al.* 1998) for the derivation of an aerosol model specifically dedicated to the Sahara region. Each valid AERONET observation, which is defined according to the same criteria as in Dubovik *et al.* (2002) and Levy *et al.* (2007), could be represented by a spectral path or trajectory in a two-dimensional space defined by the asymmetry parameter g and the single scattering albedo ω_0. This trajectory is written $(g(\lambda), \omega_0(\lambda))$ considering four AERONET wavelengths λ: 0.44, 0.67, 0.87 and 1.02 µm. The mean spectral trajectory has been estimated considering all AERONET stations available in the vicinity of the Sahara region. The corresponding mean aerosol model is shown in figure 3. This model is composed of spheroid particles whose single scattering properties are derived with the method proposed by Dubovik (2006).

4. Evaluation

The overall results of the mean relative difference $\bar{B}$ and standard deviation between satellite TOA BRFs and SIXS-V simulations over Libya4 are shown on table 2, together with the overall mean and range of $\bar{B}$ for each sensor in the common spectral bands. The range of $\bar{B}$ is computed as the difference between the maximum and minimum values of B. As can be seen, simulations performed in the 0.44 and 0.55 µm bands systematically underestimate observations. Such a clear behaviour does not occur in the other spectral intervals. However, in all common spectral bands, there is a very good consistency between AQUA-MODIS, MERIS and PARASOL radiometers, where the difference in the range of $\bar{B}$ values for each common spectral band does not exceed 1.5%, indicating that these radiometers are consistently calibrated

(*a*)

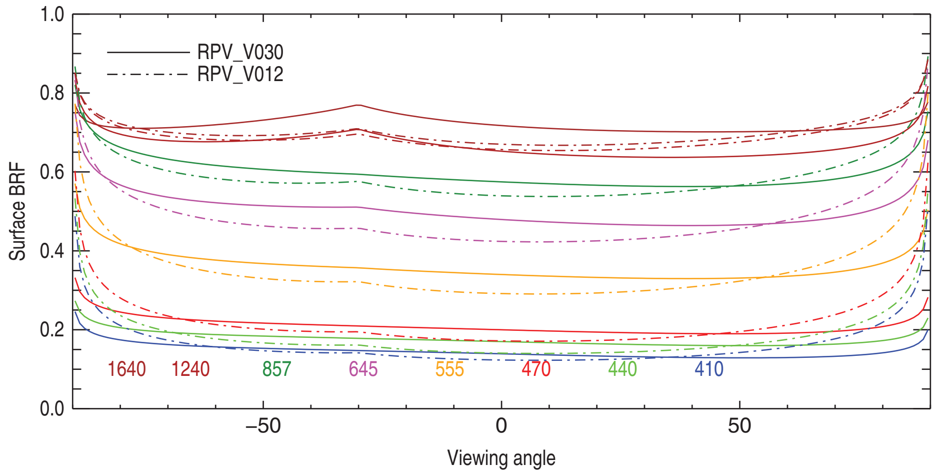

(*b*)

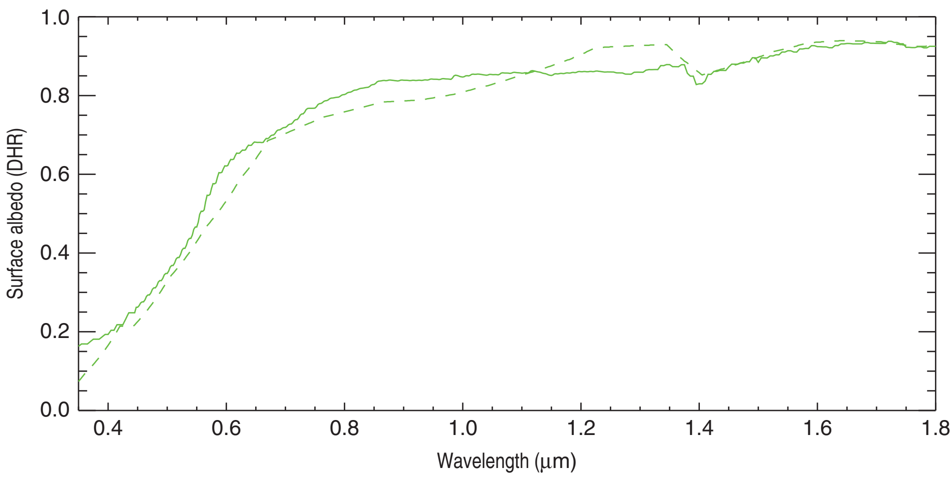

Figure 2. (*a*) Surface BRF in the principal plane over Libya4 in the following wavelengths: 410, 440, 470, 555, 645, 857, 1240 and 1640 nm. The original values are shown with dash-dotted lines. The proposed improvements are shown with solid lines. (*b*) Surface albedo (directional hemispherical reflectance (DHR)) over Lybia4. The original values are shown with dashed lines and the proposed improvements are shown with solid lines.

between themselves. VEGETATION-2 simulations overestimate TOA BRF observations to the exception of the blue band. AATSR TOA BRFs restricted to nadir camera observations are systematically lower than simulated ones. The mean $\bar{B}$ values derived considering all radiometers show that it is possible to simulate TOA BRF within 3% accuracy when enough observations are taken into account. The range of $\bar{B}$ values shows that there is still room to improve the calibration consistency among these radiometers.

We next examine the seasonal variations of the ratio $R_M(t) = r_o(t)/r_s(t)$. For that purpose, the monthly mean value of that ratio $\bar{R}_M$ has been computed during

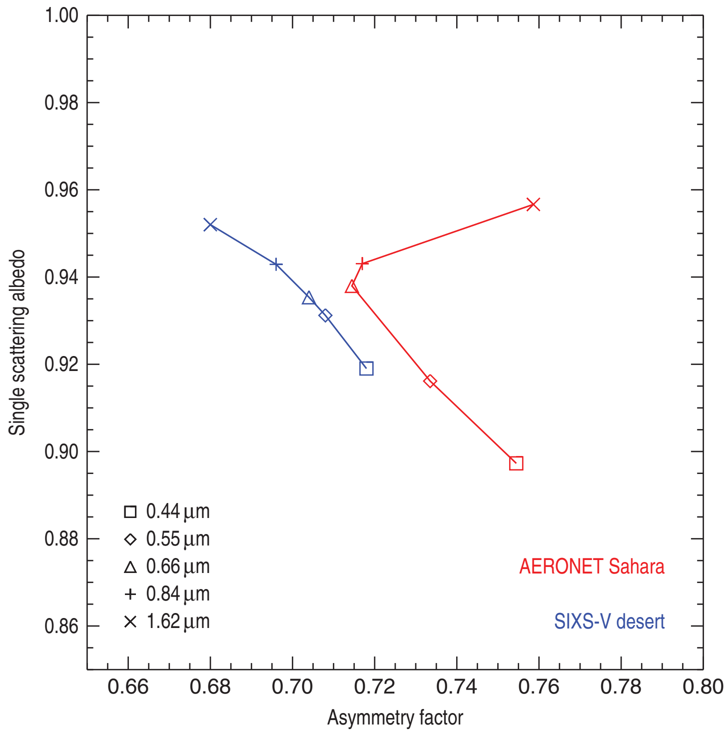

Figure 3. Representation of the new aerosol model (red) and the Shettle one (blue) in the asymmetry parameter-single scattering albedo space at the common spectral intervals. See text for details.

Table 2. Mean relative difference and standard deviation between satellite TOA BRFs and SIXS-V simulations over Libya4 during the 2006–2009 period. Positive values indicate that simulations underestimate observations. The last two lines display respectively the mean and range of the $\bar{B}$ values of each different sensor. SD is the standard deviation.

	Mean relative difference (%)					SD of relative difference (%)				
Bands (µm) sensors	0.44	0.55	0.66	0.84	1.62	0.44	0.55	0.66	0.84	1.62
VGT	0.79	–	−3.14	−2.46	−1.13	2.82	–	1.05	1.26	1.52
AATSR	–	3.89	2.81	4.21	3.82	–	1.32	1.06	1.42	0.85
PARASOL	3.08	0.71	−0.23	0.00	–	5.20	2.81	2.23	1.79	–
MODISA	3.36	2.95	0.58	1.55	2.05	1.98	1.91	1.55	1.45	1.41
MERIS	2.60	2.80	1.41	1.50	–	1.57	1.43	1.07	1.25	–
Mean	2.46	2.59	0.29	0.96	1.58					
Range	2.57	3.18	5.95	6.50	4.95					

the period of acquisition. Results are shown in figure 4 for the AQUA-MODIS instrument. The 0.41 µm band shows a small seasonal cycle as opposed to all other bands that do not exhibit any seasonal trends.

Finally, the value of $R_M(t)$ averaged over the entire period is presented in figure 5, considering now all processed bands of each radiometer. This result confirms the good

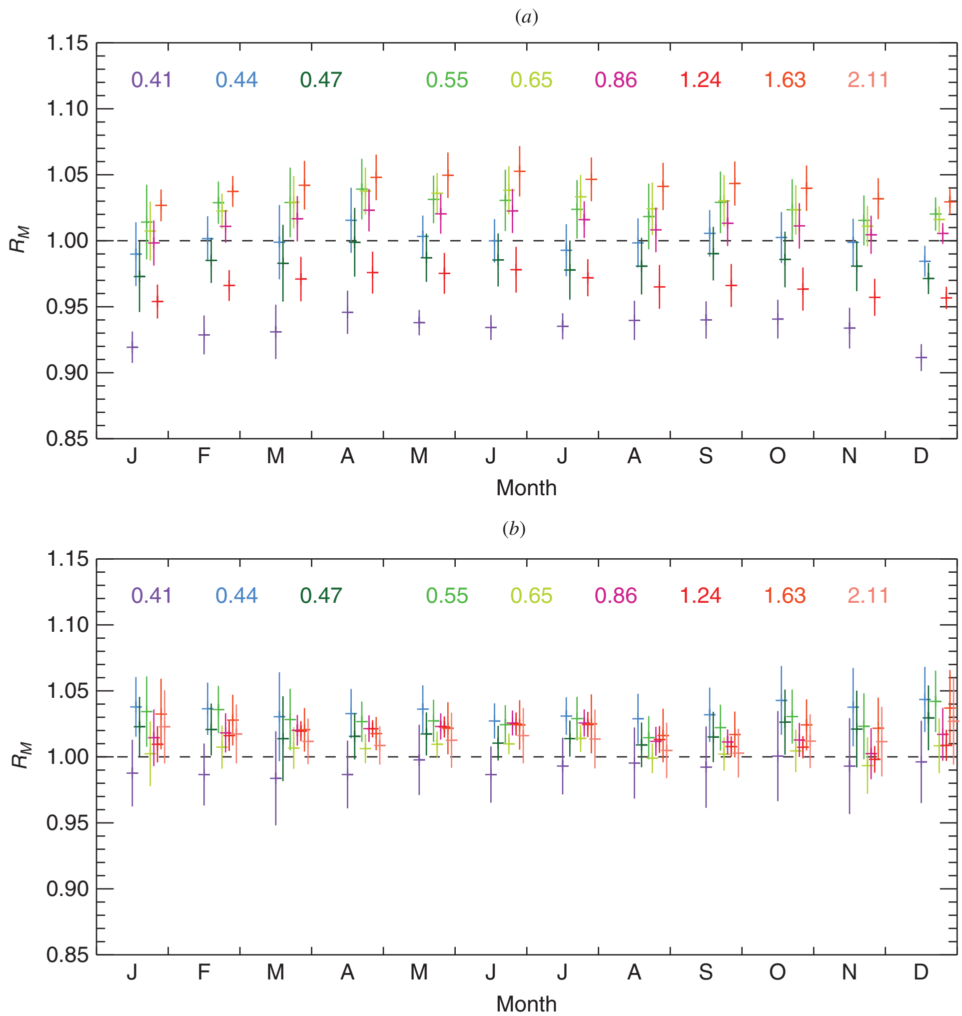

Figure 4. Monthly ration $\bar{R}_M$ (horizontal bars) between observations and simulations for the AQUA-MODIS instrument over the Libya4 site during the 2008–2010 period. The vertical bars show the standard deviation of $\bar{R}_M$ for each month. The colours represent the different processed MODIS spectral bands. (*a*) With the original surface and aerosol data set. (*b*) With the new data sets.

consistency between AQUA-MODIS, MERIS and PARASOL radiometers. There is still room for the improvement of these results in particular (*i*) in the 0.41–0.47 μm spectral region where simulations in both the 0.41 and 0.47 μm spectral bands underestimate observations and (*ii*) the observations in the 0.55 μm spectral band tends to be underestimated by simulations.

5. Conclusion

We present here an improvement of the bright desert radiative data set (Govaerts and Clerici 2004) which is used for the generation of an absolute calibration reference. This

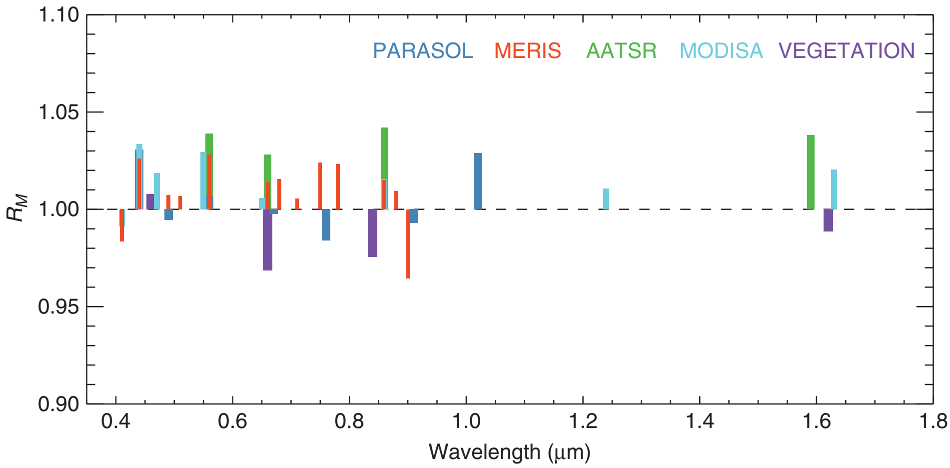

Figure 5. Value of $R_M(t)$ averaged over the entire period for each processed satellite data over the Libya4 site.

improvement is illustrated on a case study performed over Libya4. This work has been performed in the context of an evaluation of the ESA DIMITRI initiative under the umbrella of CEOS/WGCV/IVOS calibration activities. These improvements include atmospheric polarization processes, the consideration of spheroidal aerosol particles and finally the surface BRF.

It has been shown that, on the average, it is possible to simulate observations acquired by polar orbiting radiometers over Libya4 with an accuracy of 3%, the largest error being observed in the blue spectral region. The reason of this discrepancy is still an open issue that would require further works. This work also reveals differences between the calibration of these radiometers, in particular for the VEGETATION-2 and Envisat/AATSR instruments. Finally, it might be worth while to expand this work to all desert targets identified by Cosnefroy *et al*. (1997) in order to further increase the simulation accuracy, reducing the impact of uncorrelated errors among these various targets.

These improved simulated TOA BRFs represent an absolute calibration reference against which radiometers can be calibrated or their calibration compared. Such calibration reference allows also the calibration of satellite observations acquired prior to the AQUA era thanks to the very high temporal stability of the surface radiative properties. It can also be used as a reference for cross-calibration purposes, allowing to take explicitly into account difference in the spectral response and observation geometries of the various compared radiometers.

Acknowledgement
This work has been funded by BELSPO under contract 071220.

References

Bouvet, M. and Ramoino, F., 2010, Radiometric intercomparison of AATSR, MERIS, and Aqua MODIS over Dome Concordia (Antarctica). *Canadian Journal of Remote Sensing*, **36**, pp. 464–473.

Cosnefroy, H., Briottet, X., Leroy, M., Lecomte, P. and Santer, R., 1997, A field experiment in Saharan Algeria for the calibration of optical satellite sensors. *International Journal of Remote Sensing*, **18**, pp. 3337–3359.

Diner, D.J., Martonchik, J.V., Borel, C., Gerstl, S.A.W., Gordon, H.R., Knyazikhin, Y., Myneni, R., Pinty, B. and Verstraete, M.M., 1999, *Multiangle Imaging Spectro-Radiometer (MISR) Level 2 Surface Retrieval (MISR-10) Algorithm Theoretical Basis, Jet Propulsion Laboratory* (Pasadena, CA: California Institute of Technology).

Dubovik, O., 2006., Optimization of numerical inversion in photopolarimetric remote sensing. In *Photopolarimetry in Remote Sensing*, G. Videen, Y. Yatskiv and M. Mishchenko (Eds.), vol. 161, pp. 65–106 (Dordrecht: Springer).

Dubovik, O., Holben, B., Eck, T.F., Smirnov, A., Kaufman, Y.J., King, M.D., Tanre, D. and Slutsker, I., 2002, Variability of absorption and optical properties of key aerosol types observed in worldwide locations. *Journal of the Atmospheric Sciences*, **59**, pp. 590–608.

Govaerts, Y.M. and Clerici, M., 2004, Evaluation of radiative transfer simulations over bright desert calibration sites. *IEEE Transactions on Geoscience and Remote Sensing*, **42**, pp. 176–187.

Holben, B.N., Eck, T.F., Slutsker, I., Tanre, D., Buis, J.P., Setzer, A., Vermote, E., Reagan, J.A., Kaufman, Y.J., Nakajima, T., Lavenu, F., Jankowiak, I. and Smirnov, A., 1998, AERONET-A federated instrument network and data archive for aerosol characterization. *Remote Sensing of Environment*, **66**, pp. 1–16.

Kotchenova, S.Y. and Vermote, E.F., 2007, Validation of a vector version of the 6S radiative transfer code for atmospheric correction of satellite data. Part II. Homogeneous Lambertian and anisotropic surfaces. *Applied Optics*, **46**, pp. 4455–4464.

Kotchenova, S.Y., Vermote, E.F., Matarrese, R. and Klemm, Jr., F.J., 2006, Validation of a vector version of the 6S radiative transfer code for atmospheric correction of satellite data. Part I: path radiance. *Applied Optics*, **45**, pp. 6762–6774.

Levy, R., Remer, L. and Dubovik, O., 2007, Global aerosol optical properties and application to Moderate Resolution Imaging Spectroradiometer aerosol retrieval over land. *Journal of Geophysical Research*, **112**, D13210, doi:10.1029/2006JD007815.

Liou, K.N., 2002, *An Introduction to Atmospheric Radiation*, 2nd edn. (London: Academic Press).

Mellab, K., 2009, Small satellite technology to monitor the global earth: the Proba-V mission. In *Proceedings of the 33rd International Symposium on Remote Sensing of Environment (ISRSE)*, 4–8 May 2009, Stresa, Italy, p. 33. Available online at: http://www.gbv.de/dms/tib-ub-hannover/647175320.pdf

Rahman, H., Pinty, B. and Verstrete, M.M., 1993, Coupled surface-atmosphere reflectance (CSAR) model. 2. Semiempirical surface model usable with NOAA advanced very high resolution radiometer data. *Journal of Geophysical Research*, **98**, pp. 20791–20801.

Shettle, E.P. and Fenn, R.W., 1979, Models for the aerosols of the lower atmosphere and the effects of humidity variations on their optical properties. Technical report AFGL-TR-79-0214, U.S. Air Force Geophysics Laboratory.

Sterckx, S., Benhadj, I., Duhoux, G., Livens, S., Dierckx, W., Goor, E., Adriaensen, S., Heyns, W., Hoof, K.V., Strackx, G., Nackaerts, K., Reusen, I., Achteren, T.V., Dries, J., Roey, T.V., Mellab, K., Duca, R. and Zender, J., 2012, The PROBA-V mission: image processing and calibration. *Submitted to International Journal of Remote Sensing*.

Vermote, E.F., Tanré, D., Deuzé, J.L., Herman, M. and Morcrette, J.J., 1997, Second simulation of the satellite signal in the solar spectrum, 6S: an overview. *IEEE Trans actions on Geoscience and Remote Sensing*, **35**, pp. 675–686.

Vermote, E.F. and Vermeulen, A., 1999, Atmospheric correction algorithm: spectral reflectances (MOD09). Algorithm Technical Background Document (ATBD). Available online at: http://modis.gsfc.nasa.gov/data/atbd/atbd_mod08.pdf (accessed January 2013).